

# Spatial Quantum State Tomography with A Deformable Mirror

K. S. Kravtsov<sup>1,2,\*</sup>, A. K. Zhutov<sup>1</sup>, and S. P. Kulik<sup>1</sup>

<sup>1</sup> *Quantum Technology Centre of Moscow State University, Moscow, Russia*

<sup>2</sup> *A.M.Prokhorov General Physics Institute RAS, Moscow, Russia*

(Dated: September 16, 2019)

Quantum tomography is an essential experimental tool for testing any quantum technology implementations. Transverse spatial quantum states of light play a key role in many experiments in the field of quantum information as well as in free-space optical communications. In this letter we propose and experimentally demonstrate the tomography of spatial quantum states with a deformable mirror. It may be used to significantly outperform the conventional method with a spatial light modulator (SLM) in terms of speed and efficiency, at the same time providing polarization insensitive operation.

## INTRODUCTION

The tomography of a quantum state is a standard procedure of determining an unknown quantum state by performing a series of measurements over a large number of its copies [1–3]. This procedure is widely studied both theoretically and experimentally. In this letter we focus on the tomography of transverse spatial quantum states of light, which are often used as a model qudit system [4–6].

Unlike the two-dimensional case, where efficient experimental tools for quantum measurements are readily available, the realization of general measurements in higher dimensions is typically a much more complex problem. In some cases, e.g. for a composite qubit system, it is still easy to perform a *factorized* measurement [7], effectively reducing the overall task to single qubit measurements. On the contrary, higher dimensional *spatial* quantum states of light use degrees of freedom of a single particle, and so there is no universal and efficient solution for its measurement.

A lot of efforts were targeted at the development of so-called mode sorters [8–10]. They may be used for separation of different spatial modes that represent a natural (*computational*) basis for the quantum system in question. However, mode sorters formally enable only a single type of measurements, namely, measurements in the computational basis, that is obviously insufficient for a full state tomography. A typical solution for a general projective measurement is the use of a liquid crystal-based SLM for mode transformation followed by a single-mode fiber filter that performs projection of the resulting field onto the fundamental mode [11]. Although this method has been the standard technique of projective measurements in the spatial mode space, the SLM-based measurement technique has a number of significant drawbacks, namely associated with its low switching speed, poor efficiency, and polarization sensitivity.

The goal of this letter is to show that a measurement SLM may be effectively replaced by a MEMS deformable mirror, which can be switched at a much higher rate and

at the same time provide nearly lossless mode transformation and polarization insensitive operation. In the result, quantum tomography of substantially bright sources can be potentially performed at millisecond time frames and even faster, which is far from being tractable with conventional SLMs. This may find applications in real-time tomography of turbulent atmospheric channels and other non-stationary experimental environments.

We experimentally demonstrate a deformable mirror-based tomography in a 4-dimensional Hilbert space, that yields adequate fidelity of the reconstructed quantum states.

## QUANTUM TOMOGRAPHY

The goal of quantum tomography is to reconstruct an unknown density matrix  $\rho$  by a series of measurements performed on copies of the quantum state in question. According to the Born's rule the probability of observing an outcome  $\gamma$  for a positive operator-valued measure (POVM)  $M$  with elements  $\{M_\gamma\}$  is  $P(\gamma|\rho) = \text{Tr}(M_\gamma\rho)$ . Experimentally obtained probabilities for a sufficient number of different POVM elements allow to calculate the desired  $\rho$ . As mentioned before, the realistic measurement technique is limited to projective measurements only, so a general POVM formalism may be reduced to the following form of  $M_\gamma$ :  $M_\gamma = |P_\gamma\rangle\langle P_\gamma|$ .

The minimum number of projectors required for a complete tomography in  $d$ -dimensional Hilbert space is  $d^2$ , which may be chosen as the set of the symmetric, informationally complete (SIC)-POVM elements. In this letter we use a redundant set of  $d(d+1)$  projectors onto elements of mutually unbiased bases (MUBs), which results in a much more symmetric array of the deformable mirror states.

When it gets to experimental realization of projective measurements especially with a continuous deformable mirror, actual projectors may substantially differ from the designed ones in terms of both efficiency and fidelity. In fact, lossless projections onto MUB elements is impos-

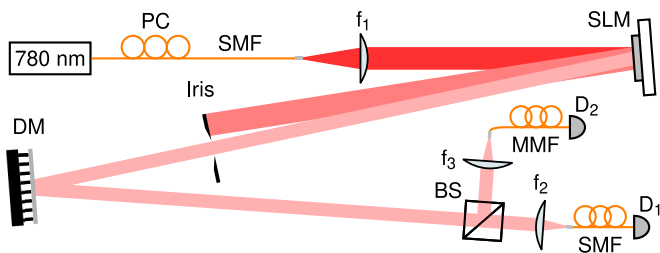


FIG. 1. Experimental setup. PC — polarization controller, SMF — single-mode fiber, DM — deformable mirror, BS — symmetric beam splitter, MMF — multi-mode fiber;  $D_{1,2}$  — single photon avalanche detectors.

sible to realize even with a perfect phase mask. Thus, before the actual state tomography one needs to perform the so called *detector tomography*, to find the actual projectors that take place in the experiment [12, 13].

### EXPERIMENTAL REALIZATION

In our demonstration we work with the following set of Hermite-Gaussian modes constituting the computational basis:  $HG_{00}$ ,  $HG_{01}$ ,  $HG_{10}$ , and  $HG_{11}$ , so the dimension of the associated Hilbert space is  $d = 4$ .

The experimental setup used in our realization is shown in Fig. 1. State preparation is realized with an SLM using the conventional mode synthesis technique described in [14]. The zero order diffraction is blocked by an iris diaphragm placed at a distance of around 1 meter from the SLM. The tomography stage is implemented with a Boston Micromachines Mini-3.5 deformable mirror (DM) consisting of 32 active elements arranged as a 6x6 matrix with missing corners. The resulting light field is focused into the single-mode fiber (SMF), delivering it to the single photon avalanche detector (SPAD). As the rate of photons in the synthesized modes varies with the mode, a reference channel with a multi-mode fiber (MMF) is added with a symmetric beamsplitter in the optical path.

The working wavelength is 780 nm, and the beam waist parameter of HG beams is  $w_0 = 0.9$  mm. As the distance between the SLM and the DM of 1.92 m is comparable with the Rayleigh range of  $z_R = 3.26$  m, the SLM hologram was adjusted to set the beam waist right at the DM plane. Besides the apparent changes of the phase curvature and the hologram size, this also requires proper accounting of the Gouy phase to get correct relative phases for superpositions of modes.

As mentioned before, for the tomography we use all 5 MUBs with 4 basis states in each as shown in Fig. 2. The states of the deformable mirror are optimized for the most efficient coupling of these 20 MUBs elements into the SMF. The basic idea is to rectify the phase, thus attaining the best overlap of the resulting field with the

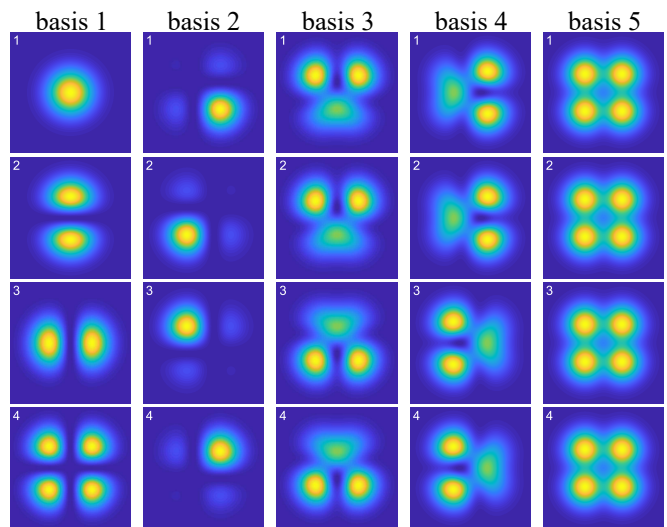


FIG. 2. Spatial distribution of amplitudes for all 20 MUB elements used for the tomography: 5 MUBs with 4 elements in each.

SMF mode.

In general, mode transformation in the deformable mirror may be described by a unitary matrix  $M'$  in a larger Hilbert space that includes higher order spatial modes:

$$\begin{bmatrix} a_1 \\ a_2 \\ a_3 \\ a_4 \\ a_5 \\ \vdots \\ a_n \end{bmatrix} = M' \begin{bmatrix} b_1 \\ b_2 \\ b_3 \\ b_4 \\ b_5 = 0 \\ \vdots \\ b_n = 0 \end{bmatrix}, \quad (1)$$

where we assume that the input state is limited to the dimension of  $d = 4$ .

Thus, tomography of DM states accesses only the left upper corner of the whole matrix  $M'$ :

$$M' = \begin{bmatrix} m_{11} & m_{12} & m_{13} & m_{14} & \cdots \\ m_{21} & m_{22} & m_{23} & m_{24} & \cdots \\ m_{31} & m_{32} & m_{33} & m_{34} & \cdots \\ m_{41} & m_{42} & m_{43} & m_{44} & \cdots \\ \cdots & \cdots & \cdots & \cdots & \cdots \\ \cdots & \cdots & \cdots & \cdots & \cdots \end{bmatrix}. \quad (2)$$

We will call it  $M$ . Apparently, this is a matrix with all eigenvalues  $|\lambda_k| \leq 1$ .

In the experiment we directly (up to the constant splitting ratio and the efficiencies of the detectors) measure probabilities  $P_{ij}$  of coupling into the single-mode fiber, where  $i$  is the number of the input state  $|\Phi_i\rangle$  and  $j$  is the number of the mirror setting;  $i, j \in \{1, 2 \dots 20\}$ . It equals

$$P_{ij} = |\langle \Psi_{00} | M_j | \Phi_i \rangle|^2, \quad (3)$$

where  $|\Psi_{00}\rangle$  is the fundamental mode and  $|\Phi_i\rangle$  — the MUBs elements.

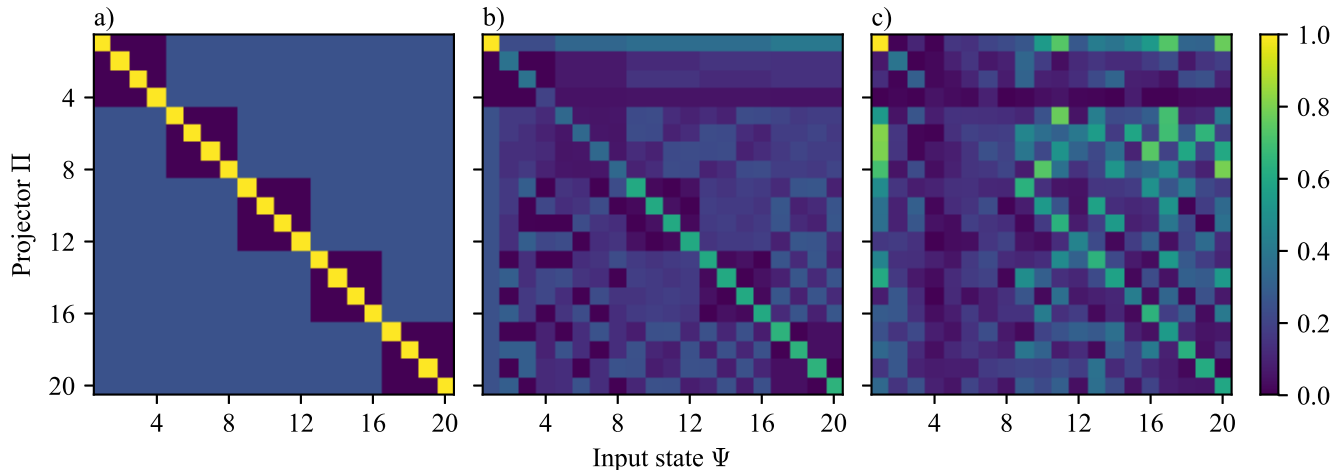


FIG. 3. A matrix of measurement results for the MUB-based protocol in a 4-dimensional Hilbert space: the probability of a state  $\Phi_i$  to pass through the projector  $\Pi_j$  a) ideal projectors onto MUB states  $\Phi_j$ ; b) ideal deformable mirror with the infinite size and resolution; c) actual measurements with our experimental setup.

If the mirror was an ideal hypothetical device for converting modes, it would be convenient to choose its settings such as  $M_j^\dagger |\Psi_{00}\rangle = |\Phi_j\rangle$ , so the  $j$ -th projector would be simply the projector onto  $|\Phi_j\rangle$ . This would result in a matrix of  $P_{ij}$  shown in Fig. 3a. In reality, a mirror even with the infinite size and resolution is not capable of such a transformation. Even the perfectly rectified phase of the field does not allow to match the amplitude profiles that leads to significant deviations of probabilities. This scenario of a perfect mirror is simulated in Fig. 3b. The actual results of the detector tomography, i.e. the experimentally measured matrix of  $P_{ij}$  is shown in Fig. 3c. Despite a significant deviation from the ideal DM, which is expected because we use only 6x6 pixels DM, the general pattern still holds and the projectors are assumed to retain the high order of symmetry to effectively perform the quantum state tomography.

To solve the overdetermined system of equations (3) for  $M_j$ , it is easier to use the more general formalism. Let the input state is described by a density matrix  $\rho$ , which is measured with the particular mirror setting  $j$ . Then the measured probability equals

$$P_j = \text{Tr}(\rho \cdot M_j^\dagger |\Psi_{00}\rangle \langle \Psi_{00}| M_j). \quad (4)$$

This equation, being effectively a HilbertSchmidt inner product for the two matrices, may be rewritten using the vectorized notation [15, 16]

$$P_j = \langle\langle \rho | M_j^\dagger |\Psi_{00}\rangle \langle \Psi_{00}| M_j \rangle\rangle. \quad (5)$$

In the detector tomography stage the input states are known and are described by the  $\rho_i = |\Phi_i\rangle \langle \Phi_i|$ , while the measurement matrix  $\Pi_j = M_j^\dagger |\Psi_{00}\rangle \langle \Psi_{00}| M_j$  is to

be found. By the construction, this matrix  $\Pi_j$  is an improperly normalized projector, i.e. has only one non-zero eigenvalue corresponding to the eigenvector  $|P_j\rangle = M_j^\dagger |\Psi_{00}\rangle$ . The eigenvalue itself shows the efficiency of the projection. For each  $j$  one needs to solve the overdetermined system of linear equations with varying  $i$ :

$$P_{ij} = \langle\langle \rho_i | M_j^\dagger |\Psi_{00}\rangle \langle \Psi_{00}| M_j \rangle\rangle. \quad (6)$$

The system is solved in the sense of a least-squares solution. Due to the presence of experimental errors especially in the case of the overdetermined system the resulting matrix  $\Pi_j$  contains more than one non-zero eigenvalue. In the detector tomography stage the minor eigenvalues are dropped to explicitly keep the form of this operator as  $\Pi_j = |P_j\rangle \langle P_j|$ .

The quantum state tomography is the reverse of the detector tomography: knowing  $\Pi_j$  and  $P_j$  for all  $js$ , one needs to solve the system (5) for the unknown  $\rho$ .

It is quite apparent that almost any  $d^2 = 16$  different DM states are sufficient for the qudit tomography. However, some sets are more optimal than others. The quantitative measure may be the ratio between the largest and the smallest singular values of the matrix formed by the set of vectorized measurement matrices  $\{|\Pi_j\rangle\rangle$ :  $\eta = \max \lambda_k / \min \lambda_k$ . Indeed, if  $\eta$  is close to 1, inverting the system (5) appears to yield the smallest uncertainty due to the experimental noise. On the contrary, very large  $\eta$ s lead to the strong propagation of small experimental noise into the solution.

The ideal case of  $\Pi_j = |\Phi_j\rangle \langle \Phi_j|$  corresponds to  $\eta = \sqrt{5} \approx 2.2$ . The infinite resolution mirror yields  $\eta \approx 5.0$ ; an ideal 6x6 mirror with independent pixels and the same pixel size as in the experiment shows  $\eta \approx 10.5$ . The measured

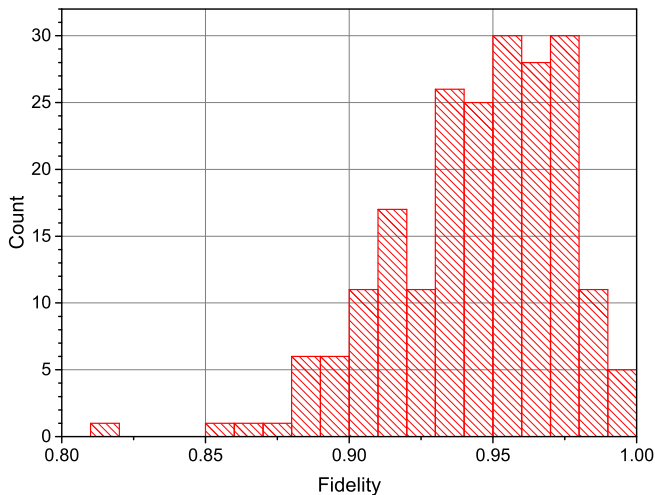


FIG. 4. Distribution of the reconstructed states fidelity for a set of 210 random pure quantum states.

matrix yields  $\eta \approx 33$ , which is not so far from the idealized case. This gives a quantitative confirmation of the claimed 'optimality' of the chosen measurements shown in Fig. 3c.

After the DM calibration matrix has been established we performed tomography of different quantum states. First of all we accomplished the tomography of the 20  $|\Phi_i\rangle$  states that yields the average fidelity with the actual states of 0.977 and the worst case fidelity of 0.940. Then, random pure qudit states were generated and their density matrices were reconstructed using the tomographic procedure. Figure 4 shows the histogram of the fidelity for the measured 210 random quantum states.

## DISCUSSION

The performed experimental demonstration shows the plausibility of the DM-based approach to spatial qudit tomography. The experimentally obtained fidelity of the reconstruction is quite similar to other tomographic experiments with spatial quantum states [11].

There are three main advantages of using a DM instead of an SLM: 1. efficiency of mode transformation; 2. polarization insensitivity; 3. speed of operation. The gain in efficiency is due to the way a liquid crystal SLM operates. Its reliable use as a phase screen is typically performed in the first order of diffraction, while all other orders, including the 0-th, lead to the signal loss. The phase shifts strongly depend on the polarization, limiting SLMs to polarized inputs only. The DM, on the contrary, reflects nearly 100% of light, giving in practice virtually no loss, but the pure polarization insensitive phase shift.

The speed of operation of a liquid crystal-based SLM is limited by a few hundred Hz, as these large molecules are not agile enough to move faster under the applied electric

field. The MEMS-based devices easily show kHz switching rates and much more [17, 18] so a properly driven DM may be able to switch states orders of magnitude faster than conventional SLMs. Another good reason for using the DM is a much more reasonable amount of data required to define a new state. In our setup we only need 32 bytes of data to completely describe the states of all 32 available actuators. More recent DMs typically have at least 100 and into a few thousand actuators, which is enough for performing tomography in a much larger Hilbert space than in our demonstration. On the other hand, a typical SLM is a megapixel class device, requiring at least 1 MB of data to define all its pixels. The data should be calculated and then transferred to the device. This by itself takes at least 3 orders of magnitude more time than transferring sub kB data for the DM, and is typically limited by the supported frame rate of the HDMI/DVI interface of a few hundred Hz.

Thus, the DM-based tomography may play a key role for the tomography of non-stationary states, where the high rate of measurements is crucial. For example, it may be used in free-space communication channels to measure the disturbance of the transmitted quantum states as well as in other dynamic experiments, where quantum states vary in time. In the same way, it could be used for the measurement of modal composition of classical bright beams of light, as in classical free-space communications.

While the advantage in the efficiency is not that striking, DMs still may replace SLM's to improve the overall detection efficiency, critical in many quantum technology demonstrations. This especially applies to the tomography of unpolarized sources.

In conclusion, we demonstrated the use of a deformable mirror for transverse spatial state tomography. Being one of the most commonly used qudit systems, spatial quantum states of light play a key role in many experiments in the field of quantum information. Their fast and reliable tomography is the cornerstone of further advancement into the field. The proposed approach allows to perform tomography orders of magnitude faster and yielding higher efficiency than with the conventional SLM-based approach. The experimentally performed tomography of randomly sampled qudit states demonstrated reasonable fidelity of reconstruction.

The development of the main concept and its partial implementation was supported by the RFBR grant No. 17-02-00966. The experiment directly relies on the detection scheme and optimization techniques developed as a part of the implementation of the state support Program of NTI Centers, namely under the the free-space quantum communications initiative.

---

\* kk@quantum.msu.ru

- [1] William K. Wootters and Brian D. Fields, “Optimal state-determination by mutually unbiased measurements,” *Annals of Physics* **191**, 363–381 (1989).
- [2] Daniel F. V. James, Paul G. Kwiat, William J. Munro, and Andrew G. White, “Measurement of qubits,” *Phys. Rev. A* **64**, 052312 (2001).
- [3] Jaroslav Řeháček, Berthold-Georg Englert, and Dagomir Kaszlikowski, “Minimal qubit tomography,” *Phys. Rev. A* **70**, 052321 (2004).
- [4] Alois Mair, Alipasha Vaziri, Gregor Weihs, and Anton Zeilinger, “Entanglement of the orbital angular momentum states of photons,” *Nature* **412**, 313–316 (2001).
- [5] Jonathan Leach, Miles J. Padgett, Stephen M. Barnett, Sonja Franke-Arnold, and Johannes Courtial, “Measuring the orbital angular momentum of a single photon,” *Phys. Rev. Lett.* **88**, 257901 (2002).
- [6] Gabriel Molina-Terriza, Juan P. Torres, and Lluís Torner, “Twisted photons,” *Nature Physics* **3**, 305–310 (2007).
- [7] G. I. Struchalin, E. V. Kovlakov, S. S. Straupe, and S. P. Kulik, “Adaptive quantum tomography of high-dimensional bipartite systems,” *Phys. Rev. A* **98**, 032330 (2018).
- [8] Gregorius C. G. Berkhout, Martin P. J. Lavery, Johannes Courtial, Marco W. Beijersbergen, and Miles J. Padgett, “Efficient sorting of orbital angular momentum states of light,” *Phys. Rev. Lett.* **105**, 153601 (2010).
- [9] Hao Huang, Giovanni Milione, Martin P. J. Lavery, Guodong Xie, Yongxiong Ren, Yinwen Cao, Nisar Ahmed, Thien An Nguyen, Daniel A. Nolan, Ming-Jun Li, Moshe Tur, Robert R. Alfano, and Alan E. Willner, “Mode division multiplexing using an orbital angular momentum mode sorter and MIMO-DSP over a graded-index few-mode optical fibre,” *Scientific Reports* **5**, 14931 (2015).
- [10] Gianluca Ruffato, Marcello Girardi, Michele Massari, Erfan Mafakheri, Bereneice Sephton, Pietro Capaldo, Andrew Forbes, and Filippo Romanato, “A compact diffractive sorter for high-resolution demultiplexing of orbital angular momentum beams,” *Scientific Reports* **8**, 10248 (2018).
- [11] N. Bent, H. Qassim, A. A. Tahir, D. Sych, G. Leuchs, L. L. Sánchez-Soto, E. Karimi, and R. W. Boyd, “Experimental realization of quantum tomography of photonic qudits via symmetric informationally complete positive operator-valued measures,” *Phys. Rev. X* **5**, 041006 (2015).
- [12] J. S. Lundeen, A. Feito, H. Coldenstrodt-Ronge, K. L. Pagnell, Ch. Silberhorn, T. C. Ralph, J. Eisert, M. B. Plenio, and I. A. Walmsley, “Tomography of quantum detectors,” *Nature Physics* **5**, 27–30 (2008).
- [13] I. B. Bobrov, E. V. Kovlakov, A. A. Markov, S. S. Straupe, and S. P. Kulik, “Tomography of spatial mode detectors,” *Opt. Express* **23**, 649–654 (2015).
- [14] Eliot Bolduc, Nicolas Bent, Enrico Santamato, Ebrahim Karimi, and Robert W. Boyd, “Exact solution to simultaneous intensity and phase encryption with a single phase-only hologram,” *Opt. Lett.* **38**, 3546–3549 (2013).
- [15] Alexei Gilchrist, Daniel R. Terno, and Christopher J. Wood, “Vectorization of quantum operations and its use,” (2009), arXiv:0911.2539 [quant-ph].
- [16] Christopher James Wood, *Initialization and Characterization of Open Quantum Systems*, Ph.D. thesis, University of Waterloo, Waterloo, Ontario, Canada (2015).
- [17] Geoff Andersen, Paul Gelsinger-Austin, Ravi Gaddipati, Phani Gaddipati, and Fasil Ghebremichael, “Fast, compact, autonomous holographic adaptive optics,” *Opt. Express* **22**, 9432–9441 (2014).
- [18] Christian C. Zhang, Warren B. Foster, Ryan D. Downey, Christopher L. Arrasmith, and David L. Dickensheets, “Dynamic performance of MEMS deformable mirrors for use in an active/adaptive two-photon microscope,” in *Adaptive Optics and Wavefront Control for Biological Systems II*, edited by Thomas G. Bifano, Joel Kubby, and Sylvain Gigan (SPIE, 2016).